Bile acid receptor TGR5 is critically involved in preference for dietary lipids and obesity

Adel Bensalem, Babar Murtaza, Aziz Hichami, Amira Sayed Khan, Hayet Oulamara, Gregory Merlen, Mustapha Berrichi, Abdel-Nacer Agli, Thierry Tordjmann, Naim Akhtar Khan

Version of Record: https://www.sciencedirect.com/science/article/pii/S0955286319306965
Manuscript_c8e729c4de506ba3f7a9a6c7231d50a2

Research article

Title:

Bile acid receptor TGR5 is critically involved in preference for dietary lipids and obesity

Authors:

Adel Bensalem[a,b], Babar Murtaza[a], Aziz Hichami[a], Amira Sayed Khan[a], Hayet Oulamara[b], Gregory Merlen[c], Mustapha Berrichi[a,d], Abdel-Nacer Agli[b], Thierry Tordjmann[c], Naim Akhtar Khan[a,*]

Authors' Affiliations :

[a] Physiologie de la Nutrition & Toxicologie, UMR U1231 INSERM/Université de Bourgogne-Franche Compté (UBFC), Dijon 21000, France.

[b] Laboratoire de Nutrition et Technologie Alimentaire (LNTA), Institut de la Nutrition, de l'Alimentation et des Technologies Agro-Alimentaires (INATAA)/Université Frères Mentouri Constantine 1 (UFMC1), 25000, Alegria.

[c] Interactions Cellulaires et Physiopathologie Hépatique, UMR U 1174 INSERM/Université Paris Sud, 91405, Orsay Cedex, Paris, France.

[d] Faculté de Pharmacie, Université Abou Bekr Belkaid, Tlemcen, Algeria.

[*] **Corresponding author:** Physiologie de la Nutrition & Toxicologie, UMR INSERM U1231, Université de Bourgogne-Franche Comté (UBFC), Dijon-21000 6, boulevard Gabriel, Dijon 21000, France. Tel.: +33 3 80 39 63 12; Fax: + 33 3 80 39 63 30.

E-mail: naim.khan@u-bourgogne.fr

Running title: TGR5 and obesity.

Financial disclosure: Nothing to disclose.

Conflict of interest: The authors declare no conflict of interest.

Author contributors: Study concept and design (NAK, TT); acquisition of data (AB, BM, GM); analysis and interpretation of data (AB, NAK, AH); collaboration and facilities (HO, ANA, MB); calcium signaling data (ASK); study supervision (NAK).

Acknowledgements: Authors are thankful to Jean François Merlin for his technical assistance for CLAMS and Eco-MRI experiments, and also to Miss Isabelle Doignon for her help perform histological work. This work was supported by grants from the French Ministry of Higher Education and Research, INSERM annual allocations and Region Bourgogne "Innovation PARI". One of the authors (AB) is thankful to Algerian Ministry of Higher Education and Scientific Research for the grant of a scholarship (PNE). BM is grateful to the Pakistan HEC for granting a PhD scholarship.

Abbreviations:

ACC1**,** acetyl-CoA carboxylase 1; CLAMS, comprehensive laboratory animal monitoring system; CPT1α, carnitine palmitoyltransferase 1α; CVP, circumvallate papillae; DPP4, dipeptidyl peptidase 4; DIO, diet-induced obese; FAS, fatty acid synthase; GLP-1, glucagon like peptide-1; HFD, High-fat diet; IL-6, Interleukin 6; IL-1β, Interleukin 1β; LA, Linoleic acid; LPS, lipopolysaccharide; ND, Normal diet; PPARα, peroxisome proliferator-activated receptor α; TBC : Taste bud cells; TGR5, Takeda G protein-coupled receptor 5; TNF-α, Tumor necrosis factor α. LCFAs: Long-chain fatty acids.

Abstract

We investigated the implication of Takeda G protein-coupled receptor 5 (TGR5) in fat preference and fat sensing in taste bud cells (TBC) in C57BL/6 wild-type (WT) and TGR5 knock out (*TGR5*$^{-/-}$) male mice, maintained for 20 weeks on a high-fat diet (HFD). We also assessed the implication of TGR5 single nucleotide polymorphism (SNP) in young obese humans. The high-fat diet (HFD) fed *TGR5*$^{-/-}$ mice were more obese, marked with higher liver weight, lipidemia and steatosis than WT obese mice. The *TGR5*$^{-/-}$ obese mice exhibited high daily food/energy intake, fat mass and inflammatory status. WT obese mice lost the preference for dietary fat, but the *TGR5*$^{-/-}$ obese mice exhibited no loss towards the attraction for lipids. In lingual TBC, the fatty acid-triggered Ca^{2+} signaling was decreased in WT obese mice; however, it was increased in TBC from *TGR5*$^{-/-}$ obese mice. Fatty acid-induced *in-vitro* release of GLP-1 was higher, but PYY concentrations were lower, in TBC from *TGR5*$^{-/-}$ obese mice than those in WT obese mice. We noticed an association between obesity and variations in TGR5 rs11554825 SNP. Finally, we can state that TGR5 modulates fat eating behavior and obesity.

Key-words: Fat, taste bud, lipids, obesity

1. Introduction

Obesity is one of the major public health challenges of the 21st century, and its prevalence is rapidly increasing throughout the world [1, 2]. The epidemic of obesity is associated with an increased risk for a number of pathologies, notably, hypertension, diabetes mellitus, gallstone and certain types of cancer [3, 4]. Multiple genetic, social, economic, and personal life-style factors play a significant role in the pathogenesis of obesity [5]. In healthy individuals, energy intake is adjusted to energy expenditure and vice versa [6]. However, there is evidence that consumption of a high-fat diet increases total energy intake, and excess dietary fat is stored [7, 8]. Several studies have demonstrated that obesity is correlated with high fat intake [9], and obese subjects present a high preference for dietary lipids [10, 11]. Moreover, obese subjects have been reported to exhibit higher thresholds for orosensory detection of fatty acids than lean subjects [12-15].

Takeda G protein-coupled receptor 5 (TGR5), also known as G-protein-coupled bile acid receptor 1 (GPBAR1) [16], membrane bile acid receptor (M-BAR) [17], or G-protein coupled receptor 131 (GPR131) [18], is the founding member of the bile acid (BA) receptor subclass of G-protein-coupled receptors [19]. TGR5 mRNA is ubiquitously expressed in humans and rodents at various levels in different tissues [20, 21]. In mice, TGR5 mRNA is detectable with very high expression in the gallbladder, white adipose tissue (WAT), brown adipose tissue (BAT), liver, intestine, lung, heart, ovary and placenta [17, 22, 23]. We have recently shown, for the first time, that human and mice taste bud cells express TGR5 mRNA [24]. We have proposed that lingual TGR5 may be the target of taste modifiers such as Zizyphin, a triterpene, that binds to lingual TGR5.

Several recent reports have suggested the implication of TGR5 in obesity. Activation of TGR5 by bile acids [25] or by a selective agonist [26] regulates glucose metabolism and energy homeostasis. Watanabe et al. [23] showed that administration of cholic acid, a bile salt, prevented insulin resistance and decreased obesity. However, no study is available on *TGR5*$^{-/-}$ under a high-fat diet condition to better understand and demonstrate its implication in obesity. Keeping in view that obesity is associated with dietary fat preference and lingual taste bud cells express TGR5, we undertook the present study in order to explore the implication of TGR5 in fat preference under normal and obese conditions in mice.

2. Materials and methods

2.1. Mice and diets

Twelve to fourteen week old wild-type (WT) or TGR5 knock out (*TGR5*$^{-/-}$) male mice of C57BL/6 genetic background were used in the present study. The WT littermates were generated from the breeding of heterozygotes *TGR5*$^{-/-}$ mice. *TGR5*$^{-/-}$ and their wild type littermates were initially provided by Merck Research Laboratories (Kenilworth, USA) as mentioned elsewhere [22]. The mice were housed in Central Animal Care facility of the Université de Bourgogne Franche-Comté, France. Mice were maintained on standard laboratory chow and water *ad-libitum,* prior to the start of study. WT and *TGR5*$^{-/-}$ mice were divided into two groups. One group (n=6) was fed with standard laboratory chow and the other group (n=6) was fed with high-fat diet (HFD). The standard diet contained 13.5% fat energy (A03, Scientific Animal Food & Engineering, Augy, France) whereas, HFD consisted of 60% of fat energy. The HFD was prepared every day, using A03 flour, palm oil and cholesterol as previously described [27]. Body weight was measured weekly until the 20th week of the study. Food intake was calculated daily by measuring the weight of food remaining in the feeding cups. At the end of the study, the animals were fasted overnight and sacrificed under anesthesia with isoflurane. Liver, intestine and white adipose tissue (WAT) were removed, washed with sterile cold saline (w/v, 0.9%) solution, immediately frozen in liquid nitrogen and stored at -80°C until use. All procedures were conducted in accordance with French guidelines for the use and care of laboratory animals (approval codes B1010 and C1011) and experimental protocols were approved by the animal ethical committee of the Université de Bourgogne Franche-Comté, France.

2.2. Determination of blood biochemical parameters

Blood was withdrawn by the cardiac puncture from all the animals, under fasting conditions, in heparinized tubes. Plasma was obtained after centrifugation of blood (5000*g* x 10 min, 4°C). The concentration of total cholesterol was determined by colorimetric enzymatic test (Cat. No. 113009910026, DiaSys, Germany). The plasma triglycerides (TG) were determined by colorimetric enzymatic test using glycerol-3-phosphate-oxidase (Cat. No. 157109910012, DiaSys, Germany). Insulin concentrations were determined by ELISA (Cat. No. EZRMI-13K, EMD Millipore, USA). Glycemia was measured by employing OneTouch ULTRA Glucometer (LifeScan, Johnson and Johnson, USA). Homeostasis model assessment-insulin resistance (HOMA-IR) was calculated according to the formula: insulin (µUI/mL) x glucose (mg/dL)/405, in fasting condition.

2.3. *Intra-peritoneal glucose tolerance test*

To conduct intra-peritoneal glucose tolerance test (IPGTT), the mice were fasted for approximately 16 hours, and fasting blood glucose levels were determined before a solution of glucose was administered by intra-peritoneal injection (2g/kg body weight). Glucose levels were measured in tail blood at different time points for 2 hours.

2.4. *Analysis of lean and fat mass by Eco-MRI*

Body lean and fat mass were analyzed by EchoMRI 500 (EchoMRI, Houston, Texas). After 20 weeks of feeding, mice were acclimatized to the EchoMRI analyzer for at least 12 h before measurement. Scans were taken by placing animals in a thin-walled plastic cylinder (3 thick, 6.8 cm inner diameter), with a cylindrical plastic insert added to limit the movement of the animals. Within the tube, the animals were briefly subjected to a low-intensity (0.05 Tesla) electromagnetic field to measure fat mass, lean mass, free water, and total body water, as described elsewhere [28].

2.5. *Hepatic cholesterol and triglyceride measurements*

Liver Samples (25-50 mg) were homogenized in 9 ml of 2:1 chloroform:methanol mixture. The homogenate was combined with 3ml of methanol, vortexed, and centrifuged (3000*g* x 15 min). 8.25 ml of supernatant was transferred to a new glass tube, containing 4 ml of chloroform and 2.75 ml of 0.73% NaCl, and the resulting mixture was vortexed for 30 s and centrifuged (3000*g* x for 3 min). The lower phase was evaporated and re-suspended in 1 ml of fresh isopropanol [29]. Total cholesterol and triglyceride (TG) levels were determined by colorimetric enzymatic methods (DiaSys, Germany).

2.6. *Histological analysis*

After the sacrifice, liver tissues were collected, fixed in 10% (v/v) neutral-buffered formalin, embedded in paraffin and 5–6 μm thick sections were stained by Hematoxylin-Eosin-Safran (HES) dyes. Oil Red-O (ORO) staining was performed on liver cryosections. Slides were observed under a light microscope.

2.7. *mRNA detection by Real Time-quantitative PCR (RT-qPCR)*

Total RNA from liver, intestine (jejunum) and white adipose tissues (WAT) was extracted by Trizol (Invitrogen), and then treated with DNAase (RNAase-free, Qiagen) and reverse transcribed with iScript cDNA synthesis kit (Bio-Rad, USA). RT-qPCR amplification was performed in StepOnePlus™ Real-Time PCR System (Applied biosystems) by using predesigned primers and SYBR® Green PCR Master Mix (Life Technologies). Primers used are mentioned in Supplementary Table 1. The relative gene expression was determined using ΔΔCt method.

2.8. *Plasma LPS determination*

Plasma LPS was separated by reverse-phase HPLC and quantitated by MS/MS spectrometry, as described before [30]. Briefly, free fatty acids were extracted with 600 µl of distilled water and 5 ml of hexane. Fatty acid separation was performed in an Infinity 1200 HPLC binary system (Agilent), equipped with a Poroshell 120 EC C18 100 × 4.6 mm 2.7 µm column (Agilent) set at 30 °C. The further quantification of LPS involved mass spectrometer.

2.9. Two-bottle preference test for lipid or sweet solutions

Spontaneous preference test for lipid or sweet solutions was investigated by a 2-bottle choice test. WT and *TGR5*$^{-/-}$ mice were deprived of water for six hours prior to the test. Then, mice were allowed to choose between two solutions, containing either 0.2% (v/v) linoleic acid (LA) or vehicle (0.3% xanthan gum). In another set of experiment, we replaced LA by canola oil (0.2%, v/v). We also conducted an experiment wherein mice were allowed to choose between a sucrose solution (4%, w/v) or control solution (tap water). The intake of each solution was determined by weighing the feeders before and after 12 hours of the exposure.

2.10. Taste bud isolation from circumvallate papillae

Circumvallate papillae (CVP) from WT or *TGR5*$^{-/-}$ mice were isolated according to previously published procedures [31]. In brief, the lingual epithelium was separated from connective tissue by enzymatic dissociation (elastase and dispase mixture, 2 mg/ml each in Tyrode buffer: 140 mM NaCl, 5 mM KCl, 10 mM HEPES, 1 mM $CaCl_2$, 10 mM glucose, 1 mM $MgCl_2$, 10 mM Na pyruvate, pH 7.4), and papillae were dissected under a microscope. The taste bud cells (TBC) were further isolated and subjected to primary culture as described previously [31], and were used for hormonal assays and calcium signaling as described here-after.

2.11. Measurement of GLP-1 and PYY in plasma and supernatants of cultured mouse TBC

The TBC isolated, from CVP of WT or *TGR5*$^{-/-}$ mice, were incubated for 2 h at 36°C in an oxygenated medium containing dipeptidyl peptidase 4 inhibitor (DPP4i) at 0.1% (w/v) to prevent the degradation of GLP-1, and 33 μM fatty acid-free BSA or 200 μM linoleic acid [32]. Similarly, an appropriate amount of DPP4i (EMD Millipore Cat No. DPP4) was added to blood samples immediately after collection according to manufacturer's directions (Millipore) to prevent degradation of blood GLP-1. The active GLP-1 content in culture medium and plasma was quantified by ELISA (EMD Millipore, Cat. No. EGLP-35K, USA). To increase the sensitivity of ELISA, 10 pM of GLP-1 standard was added into each well before doing any assay, according to the manufacturer's recommendations (Millipore). The PYY concentrations in plasma and supernatants of cultured mouse TBC were determined by ELISA as per instructions of the furnisher (ELISA Kit for PYY, Product No. CEB067Mu, Cloud Clone Corp, USA).

2.12. Measurement of intracellular free Ca^{2+} concentrations, $[Ca^{2+}]i$

The increases in free intracellular calcium concentrations, $[Ca^{2+}]i$, were determined as described elsewhere [33]. Briefly, TBC isolated from mouse CVP were seeded onto Willico-Dish wells and, after 24 hrs, were incubated with 1 μM Fura-2/AM for 30 min in loading buffer containing: 110 mM, NaCl; 5.5 mM, KCl; 25 mM, $NaHCO_3$; 0.8 mM, $MgCl_2$; 0.4 mM, KH_2PO_4; 0.33 mM, Na_2HPO_4; 20 mM, HEPES; 1.2 mM, $CaCl_2$; and the pH was adjusted to 7.4. The changes in intracellular free Ca^{2+} concentrations, $[Ca^{2+}]i$, were

monitored using a Nikon microscope (TiU) equipped with EM-CCD (Luca-S) camera and S-fluor 40X oil immersion objective (Nikon, Tokyo, Japan). The $[Ca^{2+}]i$ was expressed as ratio, calculated as the difference between the peak F_{340}/F_{380}. All test molecules were added in small volumes with no interruption in recordings.

2.13. In vivo metabolic analysis

Metabolic monitoring was performed in WT and *TGR5*$^{-/-}$ mice using a Comprehensive Laboratory Animal Monitoring System (CLAMS, Columbia Instruments, Columbus, OH). Physical activity and whole-body metabolic profile were simultaneously measured by infrared beam breaks and indirect calorimetry, respectively. Oxygen consumption rate (VO_2, ml/kg/hr) and carbon dioxide production (VCO_2) were measured. Respiratory exchange ratio (RER = VCO_2 / VO_2) was calculated by Oxymax software (v. 4.70) to estimate relative oxidation of carbohydrate (RER = 1.0) versus fat (RER approaching 0.7), not accounting for protein oxidation; rates of energy expenditure (EE) were calculated, VO_2 x (3.815 + (1.232 x RER)) [34], and normalized for metabolically adjusted weight (Kcal/H/25g AMM). During experiment, mice had free access to water and to food *ad libitum* with ND or HFD.

2.14. Recruitment of human participants and TGR5 genotyping

The healthy (n=54) and obese (n=73) children (age= 9.13± 1.17 years) were recruited at Primary Health Care Center of Tlemcen district (Algeria) by employing a multi-stage cluster random sampling method (Supplementary Table 2). Written informed consent was obtained from parents of participants prior to inclusion in the study. A special official permission was taken from the Inspectors' of Schools (Tlemcen District). All procedures of recruitment of human participants conformed to standard guidelines of the Code of Ethics of the World Medical Association (Declaration of Helsinki) for experiments involving humans, and were reviewed and approved by the Regional ethical committee.

The Genomic DNA was extracted from 100 ml of human whole blood by using Wizard® Genomic DNA Purification Kit (Promega, Fitchburg, WI, USA), and stored at -80°C until further use. Genotyping for TGR5 SNP rs11554825 (located in chromosome 2q35 position 218 834 054, exon 1) was performed using TaqMan SNP Genotyping Assays (Applied Biosystems, Foster City, CA, USA) as per the manufacturer's instructions. Following PCR amplification, end reactions were analyzed using TaqMan Genotyper Software (Applied Biosystems). According to this genotyping, C is the major allele and T the minor allele.

2.15. Statistical analysis

For statistical analysis, Statistica software (version 4.1, Statsoft, Paris, France) was used. Data represent the values as mean ± SEM. The significance of the differences between values was determined by one way analysis of variance, followed by least-significant-difference (LSD) test. For all the tests, the significance level chosen was $p < 0.05$.

3. Results

3.1. HFD triggers higher obesity in TGR5$^{-/-}$ mice than WT animals

In the present study, both the strains of mice were maintained on a normal diet (ND) or a high-fat diet (HFD). The latter diet was rich in saturated fatty acids (Supplementary Table 3). All mice maintained on a HFD gained weight continuously as a function of time (Fig. 1A). Interestingly, *TGR5*$^{-/-}$ mice fed a HFD exhibited significantly higher weight gain than WT animals fed the same diet. However, no significant difference was observed between weights of WT and *TGR5*$^{-/-}$ mice maintained on a ND. Mice fed a HFD exhibited lesser food intake than ND animals. Interestingly, *TGR5*$^{-/-}$ mice fed a HFD consumed significantly more food and energy (Fig. 1B, C), exhibited lower energy expenditure (Fig. 1D) and had higher body fat mass (Fig. 1E) than WT obese mice. No difference was observed for lean mass in both the strains of mice fed a HFD or a ND (Fig. 1F).

3.2. TGR5$^{-/-}$ obese mice develop severe insulin resistance, hyperlipidemia and liver steatosis

The obese (WT and *TGR5*$^{-/-}$) mice exhibited higher concentrations of fasting glucose and insulin, and had higher HOMA-IR than ND fed WT and *TGR5*$^{-/-}$ mice (Fig. 2A-C), though glycemia and HOMA-IR were more marked in *TGR5*$^{-/-}$ obese mice than WT obese animals. As far as intra-peritoneal glucose tolerance test (IPGTT) is concerned, the animals of both the strains fed a HFD had higher levels of glucose than those fed the ND (Fig. 2D). Though a tendency of a higher glucose concentration was observed in *TGR5*$^{-/-}$ obese mice, but it was not significantly higher than WT obese mice. The obesity in *TGR5*$^{-/-}$ mice was associated with higher plasma and liver cholesterol and triglyceride (TG) concentrations than those in WT obese mice (Fig. 3A - E).

Moreover, *TGR5*$^{-/-}$ obese mice exhibited higher liver weights (Fig. 3C) and more marked liver steatosis than WT obese mice (Fig. 4). Both the strains of obese mice developed hepatic steatosis characterized by excessive accumulation of fat droplets in liver cells. Steatosis in WT obese mice occurred as micro-vesicular vacuoles, characterized by small, round and clear vacuoles within the cytoplasm of hepatocytes (Fig. 4A). However, hepatocytes of *TGR5*$^{-/-}$ obese mice contained large, round and clear vacuoles (macrovesicular steatosis). Oil Red O staining for neutral lipids showed that HFD markedly increased lipids accumulation in the liver of *TGR5*$^{-/-}$ mice (Fig. 4B).

3.3. Spontaneous preference for fat, but not for sweet, is altered in TGR5$^{-/-}$ mice

It is interesting to note that *TGR5*$^{-/-}$ mice, fed a ND, exhibited the same attraction for a fat-containing solution (linoleic acid or canola oil) as the ND fed WT mice in a two-bottle choice test (Fig. 5A-B). Previously, our team has demonstrated that obese mice exhibit a decreased preference for fat [35]. As expected, the WT obese mice exhibited a decreased preference for fat in these experiments. Surprisingly, the preference for fat-containing solutions was abolished in obese *TGR5*$^{-/-}$ animals (Fig. 5A-B). Sweet solutions

have been used a positive control in conditioning the animals as these solutions are very hedonic. WT and *TGR5*$^{-/-}$ mice fed ND or HFD exhibited the same preference for a sucrose-containing solution over control solution (Fig. 5C).

3.4. Linoleic acid-triggered Ca^{2+} signaling and GLP-1 release are increased, but PYY is decreased, in taste bud cells from obese TGR5$^{-/-}$ *mouse*

LA triggered an increase in $[Ca^{2+}]_i$ in cultured taste bud cells (TBC) isolated from WT mice, fed the ND, and this increase was curtailed in TBC from the same strain of mice fed the HFD (Fig. 6A,C). Interestingly, the TBC from ND fed *TGR5*$^{-/-}$ mice had lower recruitment of $[Ca^{2+}]_i$ than ND fed WT animals. However, feeding the HFD to *TGR5*$^{-/-}$ mice resulted in a higher mobilization of $[Ca^{2+}]_i$ than *TGR5*$^{-/-}$ mice fed the ND, and this increase was up to the same extent as seen in WT mice maintained on a ND (Fig. 6B,C).

GLP-1, released from cultured TBC has been shown to regulate feeding behavior, particularly in obese mice [35]. We observed that there was no difference in GLP-1 secretion in TBC from WT mice whether maintained on a ND or HFD, though TBC isolated from ND fed *TGR5*$^{-/-}$ mice exhibited low GLP-1 release (Fig. 6D). Feeding a HFD to *TGR5*$^{-/-}$ mice resulted in a high GLP-1 release up to the same extent as observed in WT mice (Fig. 6D). Interestingly, the circulating GLP-1 concentration was decreased in *TGR5*$^{-/-}$ mice whether fed a ND or a HFD (Fig. 6E). It is noteworthy that the plasma concentrations of PYY are highly decreased in *TGR5*$^{-/-}$ obese mice (Fig. 6 insert, left panel), though LA and TGR5 agonist (RO5527239) induced-release of PYY was lesser in culture supernatants of taste bud cells from obese WT mice (Fig. 6 insert right panel).

3.5. mRNA expression of genes involved in lipid metabolism is altered in WT and TGR5$^{-/-}$ *mice*

RT-qPCR studies revealed that mRNA expression of genes involved in hepatic lipid metabolism is altered (Fig. 7). HFD fed mice had lower mRNA expression of ACC1 than ND-fed mice of either strain (Fig. 7). However, *TGR5*$^{-/-}$ mice exhibited lower ACC1 mRNA expression than WT littermates fed the same diet. HFD resulted in an increased expression of liver FAS mRNA in WT animals, but the same was decreased in *TGR5*$^{-/-}$ mice fed the same diet (Fig. 7). HFD also increased the expression of liver PPARα mRNA in WT and *TGR5*$^{-/-}$ mice than mice fed ND (Fig. 7). However, significantly lower levels of hepatic PPARα mRNA were observed in *TGR5*$^{-/-}$ fed ND or HFD when compared to their respective WT groups. HFD increased the hepatic mRNA expression of CPT1β mRNA in WT obese mice than mice fed ND. However, the opposite trend was observed in *TGR5*$^{-/-}$ obese mice where HFD decreased CPT1β mRNA expression (Fig. 7).

3.6. Inflammatory status is increased in TGR5$^{-/-}$ obese mice

Higher plasma concentrations of LPS were observed in WT mice fed a HFD than ND fed control animals (Fig. 8A). Feeding a HFD to *TGR5*$^{-/-}$ mice further increased the circulating LPS concentrations in these animals.

The inflammatory status in both the strains of mice is increased by HFD feeding (Fig. 8). IL-6 mRNA expression in liver was higher in WT mice fed HFD than ND-fed mice. Hepatic expression of IL-6 mRNA in *TGR5*$^{-/-}$ mice fed the HFD was further increased. IL-1β mRNA expression was also significantly increased in *TGR5*$^{-/-}$ mice fed a HFD than mice maintained on ND of the same strain (Fig. 8B). TNFα mRNA expression was higher in WT animals fed a HFD than ND fed controls. Conversely, *TGR5*$^{-/-}$ obese mice had higher TNFα mRNA than WT obese mice (Fig. 8B). The same tendency of high expression of pro-inflammatory cytokines was observed in intestine (jejunum) and white adipose tissues (Supplementary Figure 1).

3.7. Characterization and genotyping of human population

The characteristics of our population (54 controls, 73 obese) are shown in Supplementary Table 2. We tested the co-dominant, dominant and recessive models, we found that the recessive model is the most appropriate for comparative analysis of rs11554825 genotyping between controls and obese subjects. TGR5 SNP rs11554825 was in Hardy-Weinberg equilibrium ($p = 0.479$; $X^2 = 0.501$). We observed an association of SNP rs11554825 with obesity ($p = 0.023$). CC/CT genotype was more abundant in obese subjects than controls. However, TT genotype was more frequent in control subjects than obese subjects. This result suggests that the TT genotype confers a protection of about 71.3% in comparison with CC/CT genotype (odds ratio = 0.287 [0.093 - 0.884]).

4. Discussion

To investigate the implication of TGR5 receptor in diet-induced obesity, we maintained *TGR5*$^{-/-}$ mice and their WT littermates on normal a diet and a HFD. Our analysis suggested that HFD-induced obesity was more pronounced in *TGR5*$^{-/-}$ mice than that in WT mice, and obesity became significantly higher from the 4th week of fat-enriched regimen until 20th week of feeding. It is important to mention that there was no significant difference in total food and daily energy intake between WT and *TGR5*$^{-/-}$ mice, fed a ND. However, *TGR5*$^{-/-}$ obese mice fed the HFD had significantly more total food and energy intake than WT obese mice. There are some discrepancies as far as weight gain in *TGR5*$^{-/-}$ mice is concerned. Maruyama et al. [36] have previously demonstrated that female, but not male, *TGR5*$^{-/-}$ mice maintained on HFD became significantly heavier than those maintained on ND. Vassileva et al. [37] have reported that the body weight of *TGR5*$^{-/-}$ mice was not significantly different from their WT littermates, while fed either ND or HFD, although the HFD fed *TGR5*$^{-/-}$ male mice were slightly heavier than WT males fed the same diet. The severe obesity, observed in our study, in *TGR5*$^{-/-}$ male mice can be explained, in part, that we fed the mice the HFD for 20 weeks, while in other studies, the animals were fed the HFD only for 8 weeks. Alternatively, another explanation might be related to difference of fatty acid composition of the HFD used by us and previous investigators. Though our diet contained only 30% of fat, it was highly enriched with saturated fatty acids that constituted 45.85% of the dietary fat. The main saturated fatty acids in our study was palmitic acid (C16:0) which constituted 40.44% of the HFD. Several studies have well documented the obesogenic role of palmitic acid in humans and animals [38-40].

Interestingly, *TGR5*$^{-/-}$ obese mice had lower energy expenditure than WT obese mice. It has been reported that activation of TGR5 by the administration of natural bile acids [23] or INT-777 agonist [26] to mice increases energy expenditure and attenuates weight gain upon high-fat feeding through TGR5-mediated effects in brown adipose tissue and muscle. This metabolic effect is critically dependent on induction of the cAMP-dependent 2 iodothyronine deiodinase (D2), which converts inactive thyroxine (T4) to active 3,5,3-tri-iodothyronine (T3), a major hormone in increasing basal metabolism and thus, inducing energy expenditure. The high degree of obesity in the transgenic animals might be caused, in part, by high insulin resistance that is further marked by high HOMA-IR value. These results are in agreement with those of Thomas et al. [26] who have reported impaired glucose tolerance in *TGR5*$^{-/-}$ male mice.

Alteration in eating behavior leads to obesity, and this behavior could be modulated by several parameters [41]. Our teams is advocating the concept of a 6th sense of taste, i.e., taste for fat, that is altered in obese humans and rodents [10, 11]. No study is available on oro-sensory perception of fat in the context of TGR5 receptor, though we have shown its expression on mouse and human taste bud cells [24]. Hence, we were interested in assessing whether fat eating behaviour was altered in *TGR5*$^{-/-}$ mice. We observed that

HFD feeding induced a significant decrease in the preference for a dietary fatty acid and rapeseed oil in WT mice. However, the *TGR5*$^{-/-}$ obese mice failed to exhibit this decrease in fat preference, rather they behaved as WT animals, and this might contribute to high fat intake. In order to explain this feeding behaviour in *TGR5*$^{-/-}$ obese mice, we isolated and cultured the taste bud cells (TBC) and conducted *in vitro* experiments. We noticed that fatty acid-induced Ca^{2+} signaling was decreased in TBC from WT obese mice; however, it was increased in those from *TGR5*$^{-/-}$ obese mice. Martin et al. [32] have reported that GLP-1, released by TBC, may signal the increased orosensory perception of dietary fat. Hence, we observed that fatty acid-induced secretion of GLP-1 from TBC, but not that present in peripheral circulation, was higher in *TGR5*$^{-/-}$ obese mice than that in *TGR5*$^{-/-}$ mice fed a ND. We can state that both high Ca^{2+} signaling and high GLP-1 release by TBC from *TGR5*$^{-/-}$ obese mice might contribute to high preference for fat. Interestingly, in WT mice, the release of GLP-1 by cultured TBC was similar between the two diets as reported previously [35]. The expression of lipid sensor CD36 in TBC in either of the strains was not altered (not shown). Nonetheless, TGR5 gene deletion resulted in low plasma GLP-1 concentrations in agreement with several reports that have shown that the activation of TGR5 induces the secretion of GLP-1 from the enteroendocrine L-cells [42, 43]. Interestingly, there was no difference in circulating GLP-1 between *TGR5*$^{-/-}$ obese and *TGR5*$^{-/-}$ non-obese animals as it has been shown that GLP-1 secretion remains unchanged between obese and control healthy humans [44, 45]. As pointed out above, the intra-papillary environment is also controlling the feeding behavior via *in situ* mechanisms. To strengthen this notion, we further assessed the concentrations of PYY, the most anorexigenic peptide of the gastrointestinal tract. The circulating concentrations of PYY were highly significantly curtailed in *TGR5*$^{-/-}$ obese mice. Similarly, the fatty acid-induced and TGR5 agonist-induced release of PYY were lower than the basal concentrations. These observations suggest that low PYY will result in increased fat intake behavior via its low action on the vagus nerve (originating from intestine) or via glossopharyngeal nerve (originating from gustatory buccal epithelium). Our observations can be substantiated by a recent report that has shown that intestinal secretion of PYY is highly regulated by bile salts via their action on TGR5 [46]. However, how PYY is really released via TGR5 remains to be studied in the future.

The question arises whether there are other mechanisms that might contribute to high degree of obesity/adiposity, marked by high dyslipidemia, in *TGR5*$^{-/-}$ obese mice. It is interesting to mention that high accumulation of fat in liver of *TGR5*$^{-/-}$ mice might be due to low oxidation of lipids, caused by low PPARα and CPT1β mRNA expression. In the liver of *TGR5*$^{-/-}$ obese mice, low ACC1 and FAS transcripts will favor the conversion of acetyl-CoA to cholesterol rather than to malonyl CO-A, and this phenomenon will further contribute to increased liver lipids [47]. Indeed, palmitic acid, which represents more than 40% of the fatty acids contained in the HFD diet, might be the origin of elevated hepatic and blood TG through its conversion via acyl-CoA pathway [47] as palmitic acid has been reported to decrease fat oxidation [48].

The postprandial inflammatory response induced by food intake [49], depends on the fat content of the diet, and it is characterized by the increase in circulating concentrations of lipopolysaccharide (LPS) and chylomicrons, thus inducing mononuclear cell expression of inflammatory proteins [50]. This phenomenon is exaggerated in obese subjects [51, 52]. TGR5 is highly expressed in several immune cells, such as monocytes, alveolar macrophages and Kupffer cells [16, 53], and the activation of TGR5 has been shown to exert an anti-inflammatory response [54-56]. As expected, WT obese mice exhibited high blood LPS levels alongwith high expression of mRNA of IL-6, IL-1β and TNF-α in liver, intestine and white adipose tissues. High liver inflammation is associated with high liver steatosis in *TGR5*$^{-/-}$obese mice. Indeed, TGR5 activation contributes to hepatoprotection [22]. To cite, the *TGR5*$^{-/-}$ obese mice also had exorbitantly higher blood LPS levels and inflammatory cytokines mRNA, suggesting that the absence of TGR5 upregultes the inflammatory status.

In order to strengthen the relationship between TGR5 genetic polymorphism and obesity in human subjects, our investigations in TGR5 genotyping showed that CC/CT genotype was more prevalent in obese subjects, while the TT genotype was more prevalent in control subjects. This suggests that there is an association between the TGR5 genotype variations (rs11554825) and obesity, and the TT genotype confers more protection in comparison with CC/CT genotype.

Finally, we can sum up that our study adds a new dimension to the role of TGR5 in obesity where we demonstrate that TGR5, beside modulating lipid profile, liver and other physiological parameters including inflammatory status, also controls fat intake in the very beginning of food episode via its implication in taste bud physiology. The studies on TGR5 rs11554825 SNP further confirms its implication in obesity in young participants; however, these results should be confirmed in a large population of obese subjects in the future.

Legends of the Figures

Fig. 1. Effects of HFD on WT and *TGR5*$^{-/-}$ mice. The animals were maintained on a normal diet (ND) or a high-fat diet (HFD) for 20 weeks. The mice were weighed weekly **(A)**, and food **(B)** and food energy intake **(C)** were determined daily until 20th week of the study. Metabolic monitoring was performed using a Comprehensive Lab Animal Monitoring System (CLAMS) that simultaneously measures energy expenditure (EE) (**D**) during dark and light conditions, as explained in the Materials and Methods. Fat mass **(E)** and lean mass **(F)** were determined by Eco-MRI^{TM}. Each value represents the mean±SEM (n=6). The statistical difference between values was determined by one-way variance, followed by least-significant-difference (LSD) test. * represents the comparison between ND and HFD fed animals of both the strains ($p<0.001$). $ represents (in **A**) the comparison between HFD fed WT and *TGR5*$^{-/-}$ animals ($p< 0.01$).

Fig. 2. Effects of HFD on glucose and insulin concentrations in WT and *TGR5*$^{-/-}$ mice. The animals were maintained on a normal diet (ND) or a high-fat diet (HFD) for 20 weeks. **(A)** and **(B)** show, respectively, fasting serum glucose and insulin concentrations. (**C**) shows HOMA-IR values. Before sacrifice, intraperitoneal glucose-tolerance test (IPGTT) was also performed **(D)**, by the injection of glucose (2 g/kg-body weight). Blood was withdrawn at 15, 30, 60, 90 and 120 minutes, following glucose administration as described in the Materials and Methods. Each value represents the mean ± SEM (n=6). The statistical difference between values was determined by one-way variance, followed by least-significant-difference (LSD) test. * represents the comparison between ND and HFD fed animals of both the strains ($p<0.001$). $ represents (in **D**) the comparison between HFD fed WT and *TGR5*$^{-/-}$ animals ($p< 0.01$).

Fig. 3. Effects of HFD on lipidemia in WT and *TGR5*$^{-/-}$ mice. The animals were maintained on a normal diet (ND) or a high-fat diet (HFD) for 20 weeks and during sacrifice, a blood sample was withdrawn from the heart. Liver samples were taken to assess weight **(E)**. The cholesterol **(A, C)** and triglyceride **(B, D)** concentrations were determined as described in the Materials and Methods. Each value represents the mean ± SEM (n=6). The statistical difference between values was determined by one-way variance, followed by least-significant-difference (LSD) test. * represents the comparison between ND and HFD fed animals of both the strains ($p < 0.001$).

Fig. 4. Histological analyses of representative liver sections from WT and *TGR5*$^{-/-}$ obese mice. The animals were maintained on normal diet (ND) or a high-fat diet (HFD) for 20 weeks. After the sacrifice, liver sections of three WT mice and three *TGR5*$^{-/-}$ mice, fed a HFD were used for histological analysis. Representative pictures were obtained by staining with Hematoxylin-Eosin-Safran (HES) (**A**) and Oil Red O (**B**) as described in Materials and Methods. Magnification X10, scale bar: 100 mm.

Fig. 5. Spontaneous fat and sweet preference in WT and *TGR5*$^{-/-}$ mice. The animals were maintained on a normal diet (ND) or a high-fat diet (HFD) for 20 weeks. WT and *TGR*5 $^{-/-}$ mice were subjected to a 2-bottle choice tests for 12-h with a choice between control solution (0.3% xanthan gum) and a test solution containing either linoleic acid (LA, 0.2%, v/v; **A**) or canola oil (**B**). In (**C**), the mice were subjected to a choice between control solution (water) and sucrose (4%, w/v) as mentioned in the Materials and Methods. Values are presented as means ± SEM (n=6). The statistical difference between values was determined by one-way variance, followed by least-significant-difference (LSD) test. * represents the comparison between ND and HFD fed animals of both the strains ($p < 0.001$).

Fig. 6. Calcium signaling and GLP-1 and PYY release in TBC from WT and *TGR5* $^{-/-}$ mice. The cultured TBC (2×10^5 cells/assay) were loaded with Fura-2/AM, and the changes in free intracellular Ca^{2+} concentrations, $[Ca^{2+}]i$ (*F*340/*F*380 ratio) were recorded as described in the Materials and Methods. The figure shows the changes in $[Ca^{2+}]i$ in TBC from WT (**A**) and *TGR5*$^{-/-}$ mice (**B**), maintained or not on a HFD. **C**: shows the histograms with mean values, derived from identical experiments (n=6) as in **A** and **B**. For GLP-1 release, TBC (2×10^6 cells/assay) were incubated with or without linoleic acid (LA, at 200 µM) and after 2 h of incubation, the GLP-1 was determined in the supernatants as described in the Materials and Methods **(D)**. **E** shows the results of plasma GLP-1 in ND or HFD fed animals. **Insert** shows the concentrations of PYY in the plasma (**left panel**) and supernatants of cultured TBC, incubated with LA (50 µM) or RO5527239 (50 µM) for 1 hr (**right panel**). Data are presented as mean ± SEM (n=6). * represents the comparison between ND and HFD fed animals of both the strains ($p < 0.001$).

Fig. 7. Effects of HFD on mRNA encoding different genes of lipid metabolism in the liver of WT and *TGR5*$^{-/-}$ mice. The animals were maintained on a ND or a HFD for 20 weeks. After the sacrifice, liver samples were taken to assess mRNA expression of ACC1, FAS, PPAR-α and CPT1-β genes as explained in the Materials and Methods. Each value represents the mean ± SEM (n=6). The statistical difference between values was determined by one-way variance, followed by least-significant-difference (LSD) test. * represents the comparison between ND and HFD fed animals of both the strains ($p < 0.001$).

Fig. 8. Effects of HFD on inflammatory status in WT and *TGR5*$^{-/-}$ mice. The animals were maintained on a normal diet (ND) or a high-fat diet (HFD) for 20 weeks and during sacrifice, a blood sample was withdrawn from heart puncture to determine LPS concentrations (**A**). Liver samples were used to assess the mRNA expression (**B**) of inflammatory cytokines (IL-6, IL-1β and TNF-α) as explained in the Materials and Methods. Each value represents the mean ± SEM (n=6). The statistical difference between values was determined by one-way variance, followed by least-significant-difference (LSD) test. * represents the comparison between ND and HFD fed animals of both the strains ($p < 0.001$).

REFERENCES

[1] Smith KB, Smith MS. Obesity statistics. Prim Care. 2016;43:121-35.

[2] Ng M, Fleming T, Robinson M, Thomson B, Graetz N, Margono C, et al. Global, regional, and national prevalence of overweight and obesity in children and adults during 1980–2013: a systematic analysis for the Global Burden of Disease Study 2013. Lancet. 2014;384:766-81.

[3] Wang Y, Beydoun MA, Liang L, Caballero B, Kumanyika SK. Will all Americans become overweight or obese? Estimating the progression and cost of the US obesity epidemic. Obesity. 2008;16:2323-30.

[4] Must A, Spadano J, Coakley EH, Field AE, Colditz G, Dietz WH. The disease burden associated with overweight and obesity. J Am Med Assoc. 1999;282:1523-9.

[5] Peters JC, Wyatt H, Donahoo W, Hill J. From instinct to intellect: the challenge of maintaining healthy weight in the modern world. Obes Rev. 2002;3:69-74.

[6] Roberts SB, Fuss P, Dallal GE, Atkinson A, Evans WJ, Joseph L, et al. Effects of age on energy expenditure and substrate oxidation during experimental overfeeding in healthy men. J Gerontol. 1996;51:B148-B57.

[7] Willett WC. Dietary fat and obesity: an unconvincing relation. Am J Clin Nutr. 1998;68:1149-50.

[8] Hill JO, Melanson EL, Wyatt HT. Dietary fat intake and regulation of energy balance: implications for obesity. J Nutr. 2000;130:284S-8S.

[9] Sayed A, Serý O, Plesnik J, Daoudi H, Rouabah A, Rouabah L, et al. CD36 AA genotype is associated with decreased lipid taste perception in young obese, but not lean, children. Int J Obes. 2015;39:920-4.

[10] Besnard P, Passilly-Degrace P, Khan NA. Taste of fat: a sixth taste modality? Physiol Rev. 2016;96:151-76.

[11] Gilbertson TA, Khan NA. Cell signaling mechanisms of oro-gustatory detection of dietary fat: advances and challenges. Prog Lipid Res. 2014;53:82-92.

[12] Daoudi H, Plesník J, Sayed A, Šerý O, Rouabah A, Rouabah L, et al. Oral fat sensing and CD36 gene polymorphism in Algerian lean and obese teenagers. Nutrients. 2015;7:9096-104.

[13] Stewart JE, Newman LP, Keast RS. Oral sensitivity to oleic acid is associated with fat intake and body mass index. Clin Nutr. 2011;30:838-44.

[14] Mrizak I, Šerý O, Plesnik J, Arfa A, Fekih M, Bouslema A, et al. The A allele of cluster of differentiation 36 (CD36) SNP 1761667 associates with decreased lipid taste perception in obese Tunisian women. Br J Nutr. 2015;113:1330-7.

[15] Plesník J, Šerý O, Khan AS, Bielik P, Khan NA. The rs1527483, but not rs3212018, CD36 polymorphism associates with linoleic acid detection and obesity in Czech young adults. Br J Nutr. 2018;119:472-8.

[16] Kawamata Y, Fujii R, Hosoya M, Harada M, Yoshida H, Miwa M, et al. AG protein-coupled receptor responsive to bile acids. J Biol Chem. 2003;278:9435-40.

[17] Maruyama T, Miyamoto Y, Nakamura T, Tamai Y, Okada H, Sugiyama E, et al. Identification of membrane-type receptor for bile acids (M-BAR). Biochem Biophys Res Commun. 2002;298:714-9.
[18] Li Y, Cheng KC, Cheng J-T. GPR119 and GPR131: Functional Difference? Curr Res Diabetes Obes J. 2017;1:555566.
[19] Foord SM, Bonner TI, Neubig RR, Rosser EM, Pin J-P, Davenport AP, et al. International Union of Pharmacology. XLVI. G protein-coupled receptor list. Pharmacol Rev. 2005;57:279-88.
[20] Keitel V, Cupisti K, Ullmer C, Knoefel WT, Kubitz R, Häussinger D. The membrane-bound bile acid receptor TGR5 is localized in the epithelium of human gallbladders. Hepatology. 2009;50:861-70.
[21] Poole DP, Godfrey C, Cattaruzza F, Cottrell GS, Kirkland JG, Pelayo JC, et al. Expression and function of the bile acid receptor GpBAR1 (TGR5) in the murine enteric nervous system. Neurogastroenterol Motil. 2010;22:814-25.
[22] Merlen G, Kahale N, Ursic-Bedoya J, Bidault-Jourdainne V, Simerabet H, Doignon I, et al. TGR5-dependent hepatoprotection through the regulation of biliary epithelium barrier function. Gut. 2019:gutjnl-2018-316975.
[23] Watanabe M, Houten SM, Mataki C, Christoffolete MA, Kim BW, Sato H, et al. Bile acids induce energy expenditure by promoting intracellular thyroid hormone activation. Nature. 2006;439:484-9.
[24] Murtaza B, Berrichi M, Bennamar C, Tordjmann T, Djeziri FZ, Hichami A, et al. Zizyphin modulates calcium signalling in human taste bud cells and fat taste perception in the mouse. Fundam Clin Pharmacol. 2017;35:486-96.
[25] Houten SM, Watanabe M, Auwerx J. Endocrine functions of bile acids. EMBO J. 2006;25:1419-25.
[26] Thomas C, Gioiello A, Noriega L, Strehle A, Oury J, Rizzo G, et al. TGR5-mediated bile acid sensing controls glucose homeostasis. Cell Metab. 2009;10:167-77.
[27] Djeziri FZ, Belarbi M, Murtaza B, Hichami A, Benammar C, Khan NA. Oleanolic acid improves diet-induced obesity by modulating fat preference and inflammation in mice. Biochimie. 2018;152:110-20.
[28] Tinsley FC, Taicher GZ, Heiman ML. Evaluation of a quantitative magnetic resonance method for mouse whole body composition analysis. Obes Res. 2004;12:150-60.
[29] Turcotte L, Secco B, Lamoureux G, Shum M, Gélinas Y, Marette A, et al. Loss of hepatic DEPTOR alters the metabolic transition to fasting. Mol Metab. 2017;6:447-58.
[30] de Barros J-PP, Gautier T, Sali W, Adrie C, Choubley H, Charron E, et al. Quantitative lipopolysaccharide analysis using HPLC/MS/MS and its combination with the limulus amebocyte lysate assay. J Lipid Res. 2015;56:1363-9.
[31] El-Yassimi A, Hichami A, Besnard P, Khan NA. Linoleic acid induces calcium signaling, Src kinase phosphorylation, and neurotransmitter release in mouse CD36-positive gustatory cells. J Biol Chem. 2008;283:12949-59.
[32] Martin C, Passilly-Degrace P, Chevrot M, Ancel D, Sparks SM, Drucker DJ, et al. Lipid-mediated release of GLP-1 by mouse taste buds from circumvallate papillae: putative involvement of GPR120 and impact on taste sensitivity. J Lipid Res. 2012;53:2256-65.

[33] Dramane G, Abdoul-Azize S, Hichami A, Voegtle L, Akpona S, Chouabe C, et al. STIM1 regulates calcium signaling in taste bud cells and preference for fat in mice. J Clin Invest. 2012;122:2267-82.
[34] Lusk G. The elements of the science of nutrition. WB Saunders Compagny. 1976.
[35] Ozdener MH, Subramaniam S, Sundaresan S, Sery O, Hashimoto T, Asakawa Y, et al. CD36-and GPR120-Mediated Ca^{2+} Signaling in Human Taste Bud Cells Mediates Differential Responses to Fatty Acids and Is Altered in Obese Mice. Gastroenterology. 2014;146:995-1005.
[36] Maruyama T, Tanaka K, Suzuki J, Miyoshi H, Harada N, Nakamura T, et al. Targeted disruption of G protein-coupled bile acid receptor 1 (Gpbar1/M-Bar) in mice. J Endocrinol. 2006;191:197-205.
[37] Vassileva G, Hu W, Hoos L, Tetzloff G, Yang S, Liu L, et al. Gender-dependent effect of Gpbar1 genetic deletion on the metabolic profiles of diet-induced obese mice. J Endocrinol. 2010;205:225-32.
[38] Mancini A, Imperlini E, Nigro E, Montagnese C, Daniele A, Orrù S, et al. Biological and nutritional properties of palm oil and palmitic acid: effects on health. Molecules. 2015;20:17339-61.
[39] Chen X, Lou G, Meng Z, Huang W. TGR5: a novel target for weight maintenance and glucose metabolism. Exp Diabetes Res. 2011;2011:853501.
[40] Winzell MS, Ahrén B. The High-Fat Diet–Fed Mouse. Diabetes. 2004;53:S215-S9.
[41] Baggio LL, Drucker DJ. Biology of incretins: GLP-1 and GIP. Gastroenterology. 2007;132:2131-57.
[42] Katsuma S, Hirasawa A, Tsujimoto G. Bile acids promote glucagon-like peptide-1 secretion through TGR5 in a murine enteroendocrine cell line STC-1. Biochem Biophys Res Commun. 2005;329:386-90.
[43] Pols TW, Noriega LG, Nomura M, Auwerx J, Schoonjans K. The bile acid membrane receptor TGR5 as an emerging target in metabolism and inflammation. J Hepatol. 2011;54:1263-72.
[44] Adam TC, Westerterp-Plantenga MS. Glucagon-like peptide-1 release and satiety after a nutrient challenge in normal-weight and obese subjects. Br J Nutr. 2005;93:845-51.
[45] Feinle C, Chapman IM, Wishart J, Horowitz M. Plasma glucagon-like peptide-1 (GLP-1) responses to duodenal fat and glucose infusions in lean and obese men. Peptides. 2002;23:1491-5.
[46] Kuhre RE, Albrechtsen NJW, Larsen O, Jepsen SL, Balk-Møller E, Andersen DB, et al. Bile acids are important direct and indirect regulators of the secretion of appetite-and metabolism-regulating hormones from the gut and pancreas. Mol Metab. 2018;11:84-95.
[47] Wakil SJ, Abu-Elheiga LA. Fatty acid metabolism: target for metabolic syndrome. J Lipid Res. 2009;50:S138-S43.
[48] Kien CL, Bunn JY, Ugrasbul F. Increasing dietary palmitic acid decreases fat oxidation and daily energy expenditure. Am J Clin Nutr. 2005;82:320-6.
[49] Nappo F, Esposito K, Cioffi M, Giugliano G, Molinari AM, Paolisso G, et al. Postprandial endothelial activation in healthy subjects and in type 2 diabetic patients: role of fat and carbohydrate meals. J Am Coll Cardiol. 2002;39:1145-50.
[50] Clemente-Postigo MQ-O, MI, Murri M, Boto-Ordoñez M, Perez-Martinez P, Andres-Lacueva C, Cardona F, et al. Endotoxin increase after fat overload is related to postprandial hypertriglyceridemia in morbidly obese patients. J Lipid Res. 2012;53:973–78.

[51] Vors C, Pineau G, Drai J, Meugnier E, Pesenti S, Laville M, et al. Postprandial endotoxemia linked with chylomicrons and lipopolysaccharides handling in obese versus lean men: a lipid dose-eff ect trial. J Clin Endocrinol Metab. 2015;100:3427-35.
[52] van Nierop FS, Scheltema MJ, Eggink HM, Pols TW, Sonne DP, Knop FK, et al. Clinical relevance of the bile acid receptor TGR5 in metabolism. Lancet Diabetes Endocrinol. 2016;5:224-33.
[53] Keitel V, Donner M, Winandy S, Kubitz R, Häussinger D. Expression and function of the bile acid receptor TGR5 in Kupffer cells. Biochem Biophys Res Commun. 2008;372:78-84.
[54] Stepanov V, Stankov K, Mikov M. The bile acid membrane receptor TGR5: a novel pharmacological target in metabolic, inflammatory and neoplastic disorders. J Recept Signal Transduct Res. 2013;33:213-23.
[55] Wang YD, Chen WD, Yu D, Forman BM, Huang W. The G-Protein-coupled bile acid receptor, Gpbar1 (TGR5), negatively regulates hepatic inflammatory response through antagonizing nuclear factor kappa light-chain enhancer of activated B cells (NF-κB) in mice. Hepatology. 2011;54:1421-32.
[56] Yuan L, Bambha K. Bile acid receptors and nonalcoholic fatty liver disease. World J Hepatol. 2015;7:2811-8.

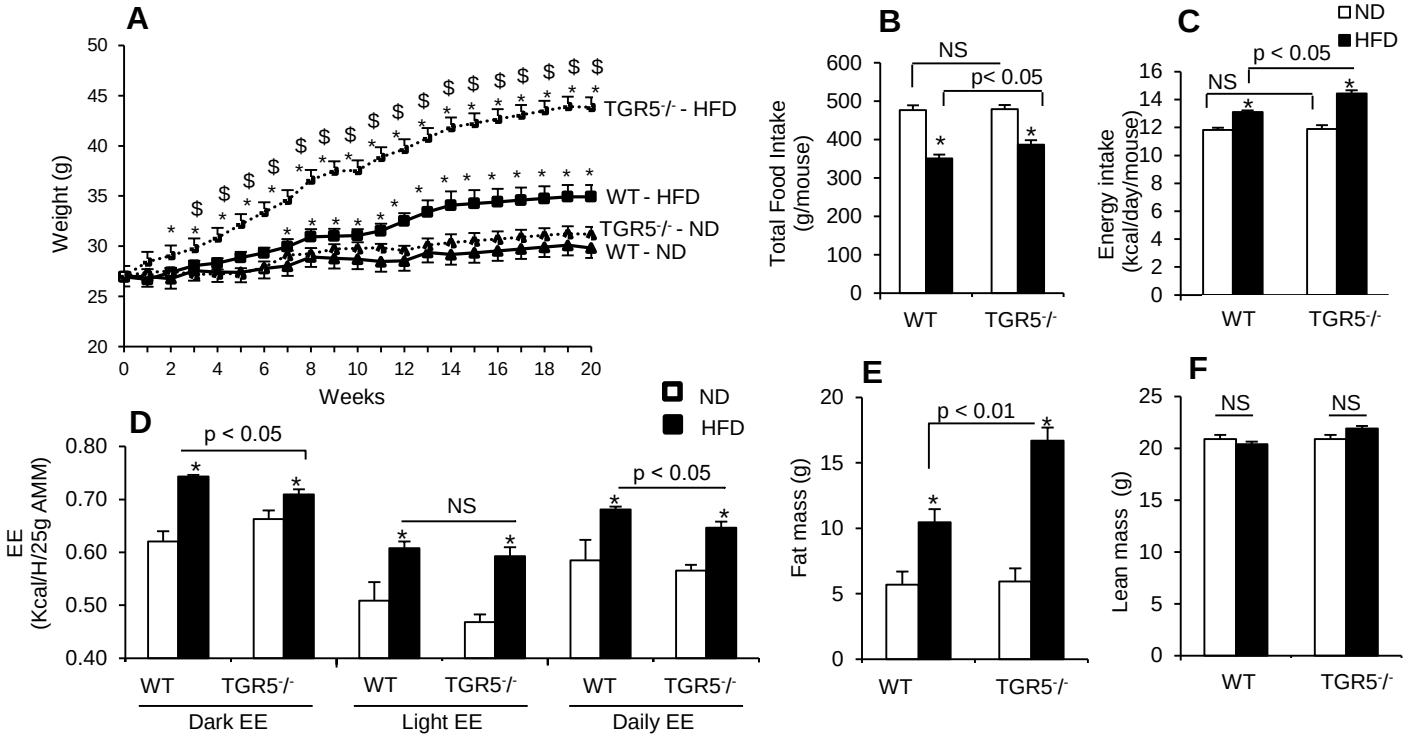
A
Weight (g)
Weeks
TGR5-/- - HFD
WT - HFD
TGR5-/- - ND
WT - ND
B
Total Food Intake (g/mouse)
NS
p< 0.05
WT
TGR5-/-
C
ND
HFD
Energy intake (kcal/day/mouse)
NS
p < 0.05
WT
TGR5-/-
D
EE (Kcal/H/25g AMM)
ND
HFD
p < 0.05
NS
p < 0.05
WT
TGR5-/-
Dark EE
Light EE
Daily EE
E
Fat mass (g)
p < 0.01
WT
TGR5-/-
F
Lean mass (g)
NS
NS
WT
TGR5-/-

Fig. 1

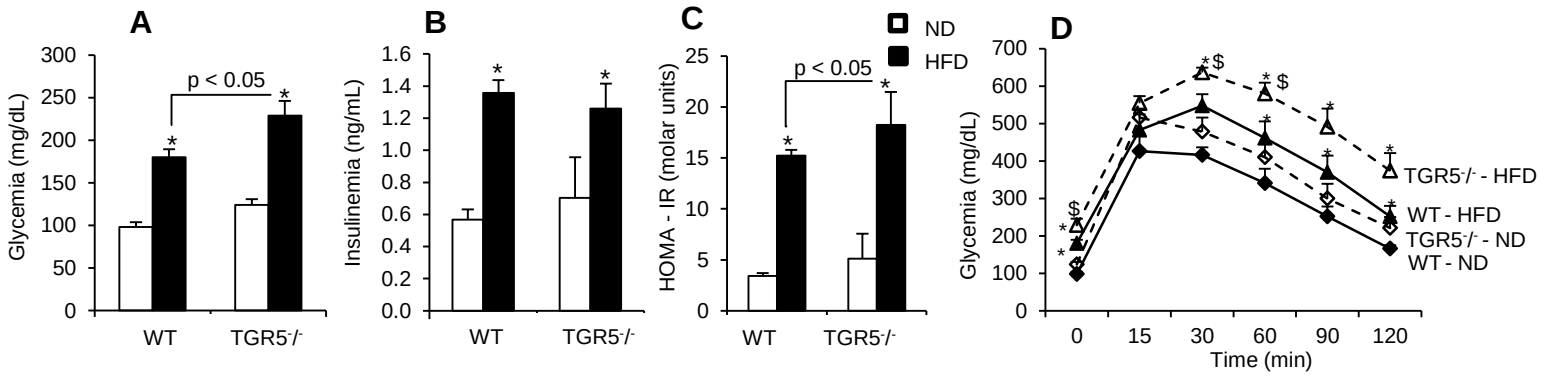
A
Glycemia (mg/dL)
300
250
200
150
100
50
0
p < 0.05
*
*
WT
TGR5-/-
B
Insulinemia (ng/mL)
1.6
1.4
1.2
1.0
0.8
0.6
0.4
0.2
0.0
*
*
WT
TGR5-/-
C
HOMA - IR (molar units)
25
20
15
10
5
0
p < 0.05
*
*
WT
TGR5-/-
ND
HFD
D
Glycemia (mg/dL)
700
600
500
400
300
200
100
0
0
15
30
60
90
120
Time (min)
TGR5-/- - HFD
WT - HFD
TGR5-/- - ND
WT - ND

Fig. 2

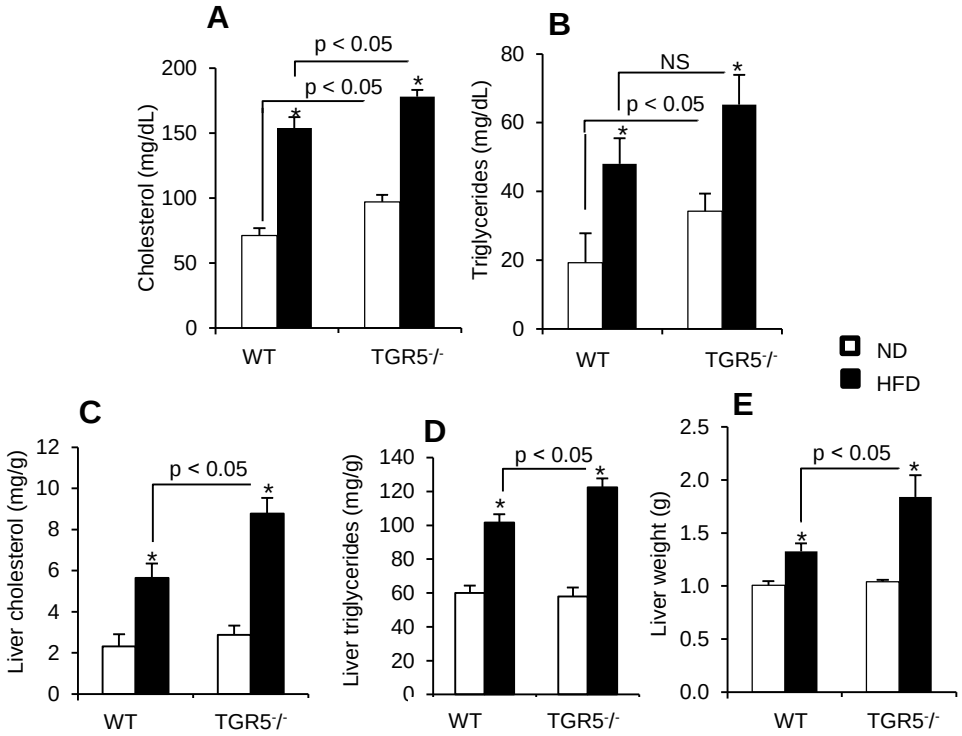
A
Cholesterol (mg/dL)
200
150
100
50
0
p < 0.05
p < 0.05
*
*
WT
TGR5-/-
B
Triglycerides (mg/dL)
80
60
40
20
0
NS
p < 0.05
*
*
WT
TGR5-/-
ND
HFD
C
Liver cholesterol (mg/g)
12
10
8
6
4
2
0
p < 0.05
*
*
WT
TGR5-/-
D
Liver triglycerides (mg/g)
140
120
100
80
60
40
20
0
p < 0.05
*
*
WT
TGR5-/-
E
Liver weight (g)
2.5
2.0
1.5
1.0
0.5
0.0
p < 0.05
*
*
WT
TGR5-/-

Fig. 3

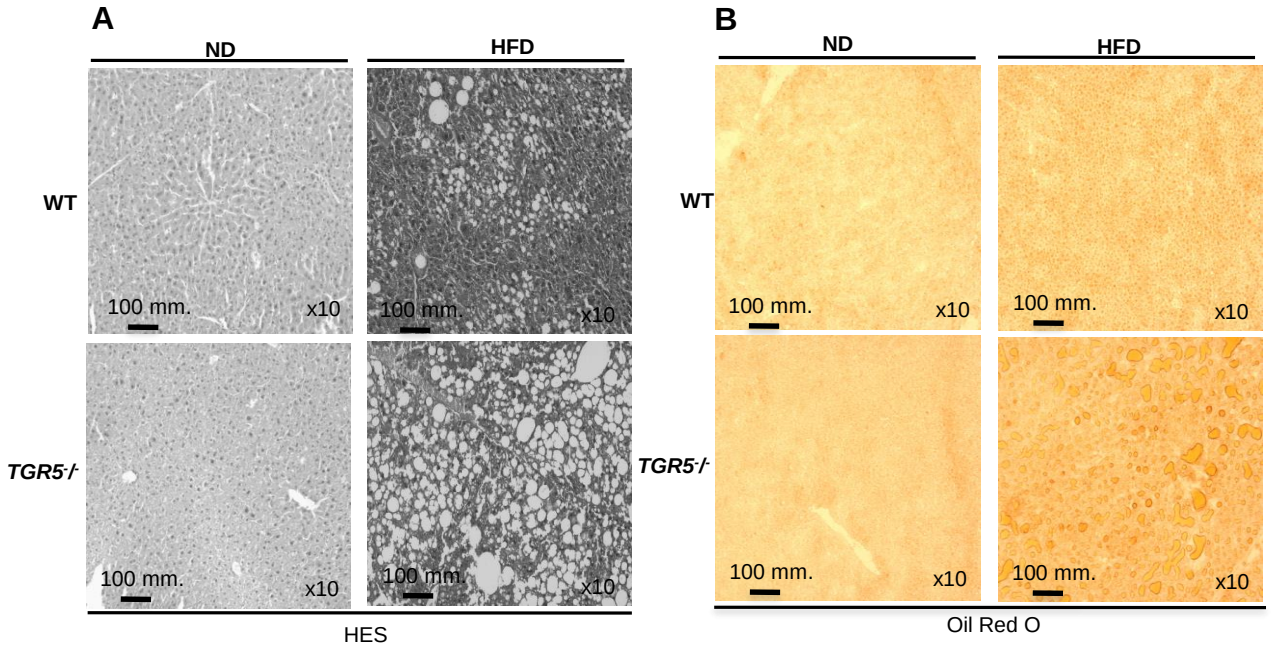
A
ND
HFD
WT
TGR5-/-
100 mm.
x10
HES
B
ND
HFD
WT
TGR5-/-
100 mm.
x10
Oil Red O

Fig. 4

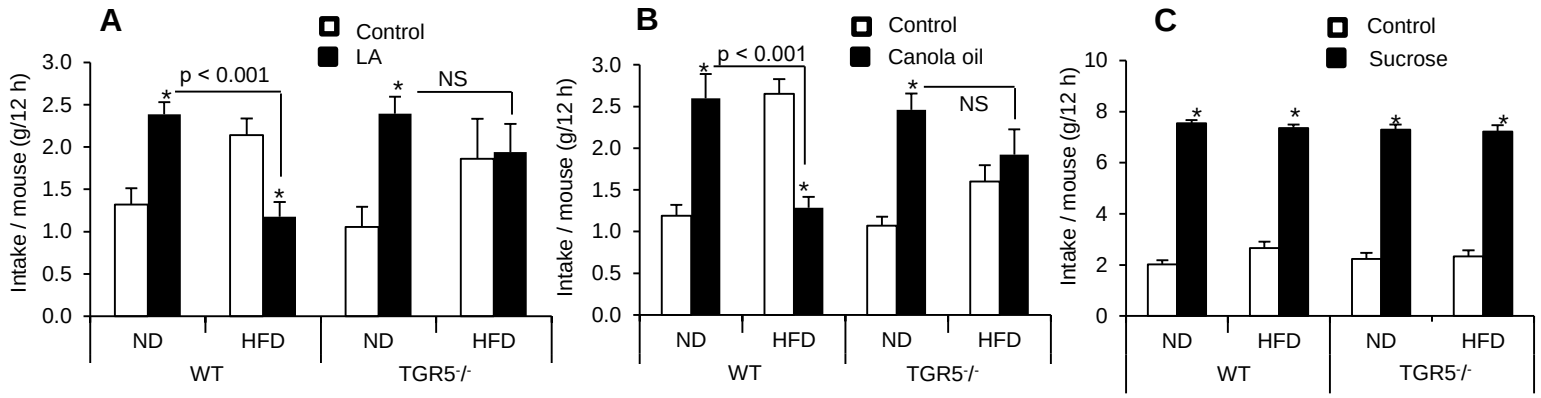
A
Control
LA
p < 0.001
NS
Intake / mouse (g/12 h)
3.0
2.5
2.0
1.5
1.0
0.5
0.0
ND
HFD
ND
HFD
WT
TGR5-/-
B
Control
Canola oil
p < 0.001
NS
Intake / mouse (g/12 h)
ND
HFD
ND
HFD
WT
TGR5-/-
C
Control
Sucrose
Intake / mouse (g/12 h)
10
8
6
4
2
0
ND
HFD
ND
HFD
WT
TGR5-/-

Fig. 5

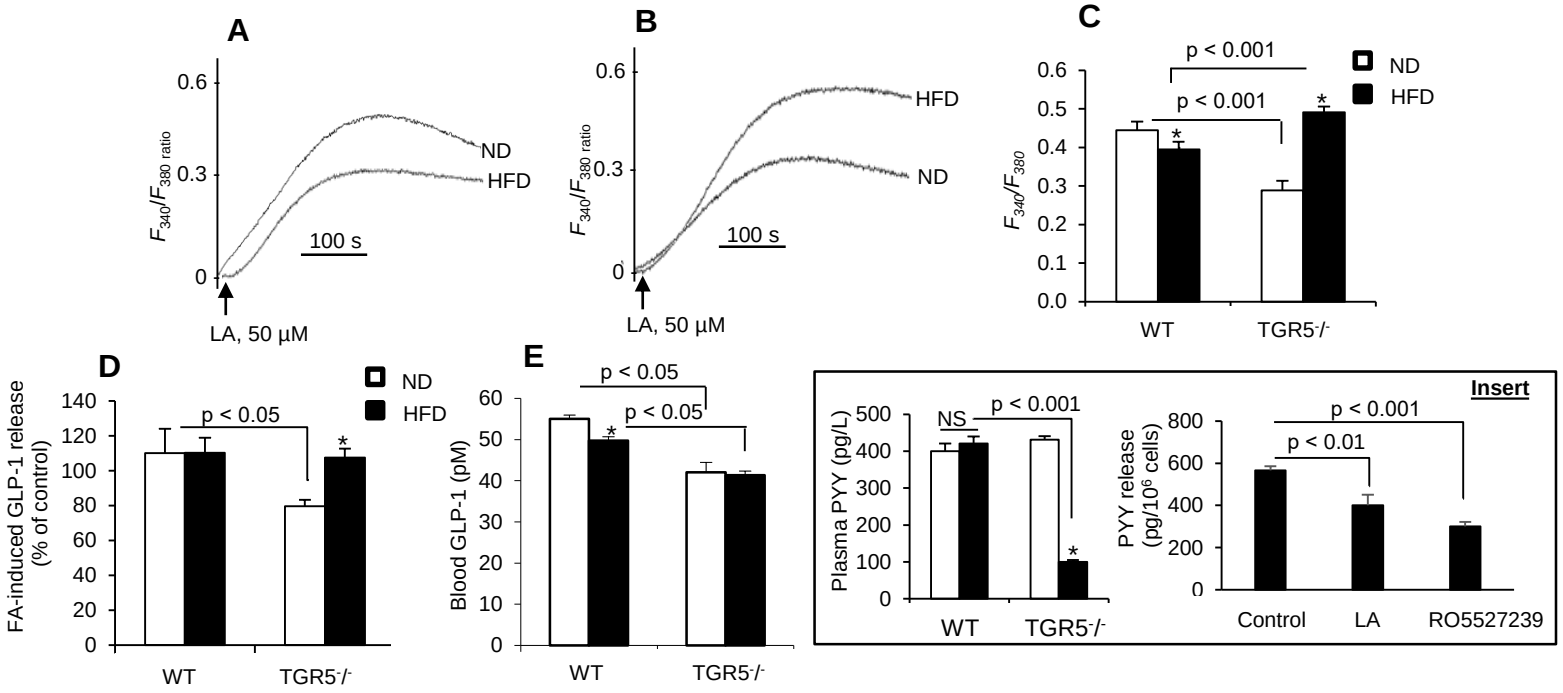
A
B
C
D
E
Insert
ND
HFD
100 s
LA, 50 µM
WT
TGR5-/-
p < 0.001
p < 0.05
p < 0.01
NS
Control
LA
RO5527239
FA-induced GLP-1 release (% of control)
Blood GLP-1 (pM)
Plasma PYY (pg/L)
PYY release (pg/10^6 cells)

Fig. 6

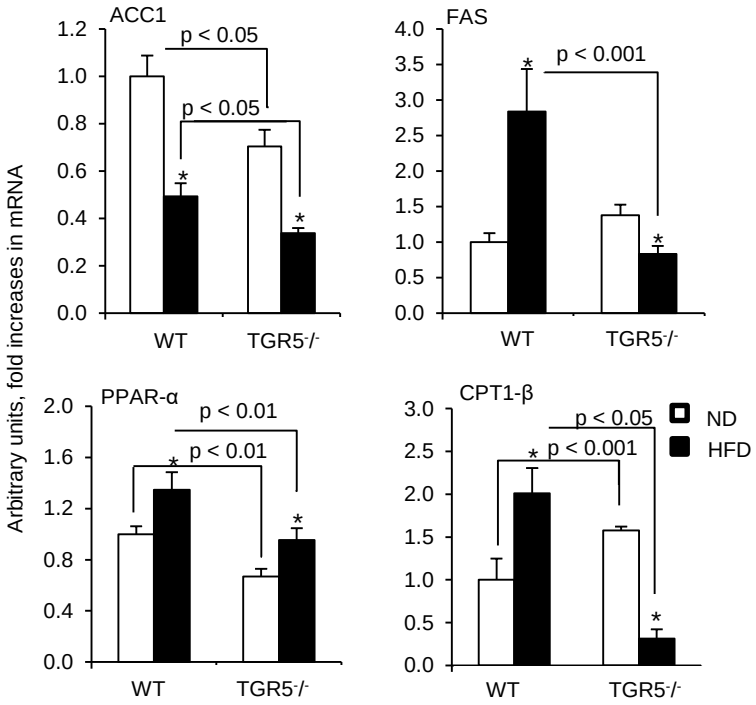
ACC1
p < 0.05
p < 0.05
FAS
p < 0.001
PPAR-α
p < 0.01
p < 0.01
CPT1-β
p < 0.05
p < 0.001
ND
HFD
Arbitrary units, fold increases in mRNA
WT
TGR5-/-

Fig. 7

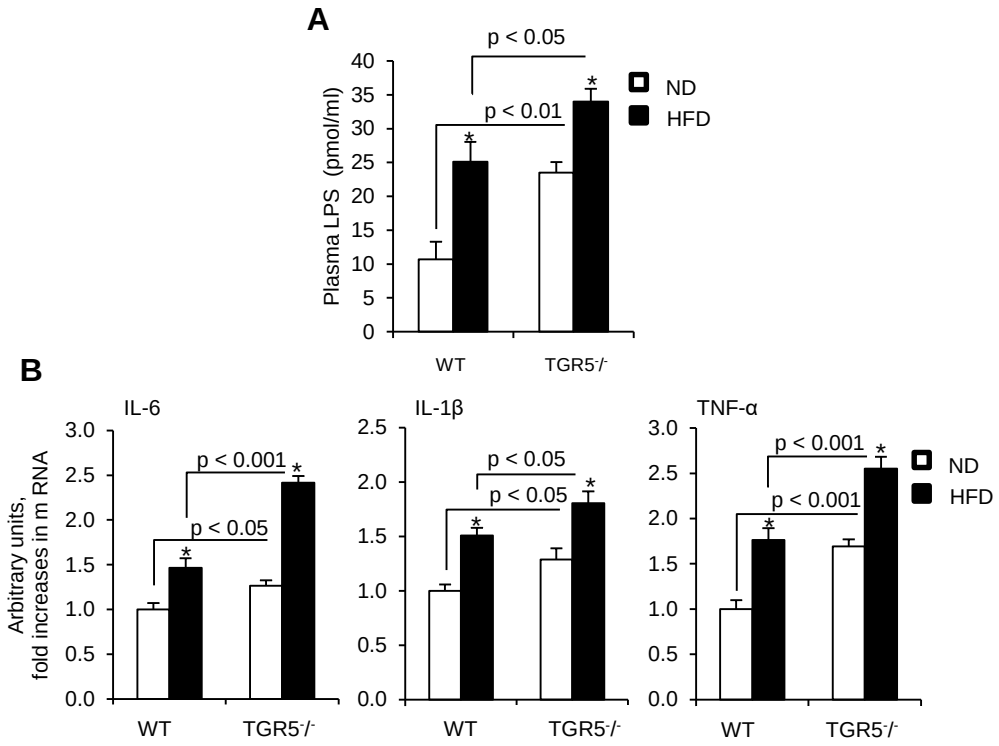
A
p < 0.05
p < 0.01
ND
HFD
Plasma LPS (pmol/ml)
40
35
30
25
20
15
10
5
0
WT
TGR5-/-
B
IL-6
IL-1β
TNF-α
Arbitrary units, fold increases in m RNA
p < 0.001
p < 0.05
p < 0.05
p < 0.05
p < 0.001
p < 0.001
ND
HFD
3.0
2.5
2.0
1.5
1.0
0.5
0.0
WT
TGR5-/-

Fig. 8